



Ligand polarizability contributes to tau fibril binding affinity

Jordan R. Jensen[†], Katryna Cisek[†], Nicolette S. Honson[‡], Jeff Kuret^{*}

Department of Molecular and Cellular Biochemistry, The Ohio State University College of Medicine, Columbus, OH 43210, USA

ARTICLE INFO

Article history:

Received 25 May 2011

Revised 7 July 2011

Accepted 11 July 2011

Available online 19 July 2011

Keywords:

Alzheimer's disease

Tau protein

Polarizability

Dispersion forces

ABSTRACT

Whole brain imaging of tau-bearing neurofibrillary lesions has the potential to improve the premortem diagnosis and staging of Alzheimer's disease. Diverse compounds with high affinity for tau aggregates have been reported from high-throughput screens, but the affinity driving features common among them have not been determined. To identify these features, analogs of compounds discovered by high-throughput screening, including phenothiazine, triarylmethine, benzothiazole, and oxindole derivatives, were tested for their ability to displace fluorescent thioflavin dyes from filaments made from recombinant tau protein or authentic paired helical filaments purified from Alzheimer's disease tissue. When representative members of all scaffolds were assayed, the rank order of binding affinity determined for synthetic and authentic filaments correlated strongly, indicating that synthetic filaments have predictive utility for ligand development. Within individual scaffold families, binding affinity was found to correlate with compound polarizability, consistent with a role for dispersion forces in mediating ligand binding. Overall, the data indicate that polarizability is an important commonality among structurally diverse tau binding ligands, and that affinity for tau aggregates can be maximized by integrating formal assessment of this parameter into ligand discovery efforts.

© 2011 Elsevier Ltd. All rights reserved.

1. Introduction

Alzheimer's disease (AD), the most common form of dementia,^{1,2} is diagnosed post-mortem by the appearance of extracellular plaques composed of amyloid beta (A β) peptide and intracellular tangles composed of tau protein aggregated into paired helical filaments (PHFs).³ Although radiotracers capable of detecting A β aggregates through whole-brain imaging have been developed,^{4–6} discovery of tau-directed imaging agents may further improve premortem assessment by identifying disease earlier in its course and by establishing its Braak stage in living cases.⁷ The search for candidate tau aggregate binding agents has relied primarily on recombinant human tau preparations induced to aggregate by the addition of anionic substances such as heparin, fatty acids, or alkyl sulfate detergents.^{8–10} The resultant tau aggregates react with fluorescent probes for cross- β -sheet conformation³ such as Thioflavin S (ThS), Thioflavin T (ThT), and primuline.^{11–13} Assay for displacement of these probes provides a rapid and high-throughput fluorescence

screen for putative tau aggregate binding ligands. A small number of compounds capable of binding tau aggregates have been discovered using these methods, including phenothiazines¹⁴ and benzothiazole derivatives,¹⁵ but the affinity driving features common among them have not been determined. Most importantly, their ability to bind authentic brain-derived PHF, which comprises six post-translationally modified tau splice variants,¹⁶ is unknown. Elucidation of the forces involved in binding small molecules to PHFs will be instrumental in the design of tau-directed radiotracers for the diagnosing and staging of AD.

To identify additional tau aggregate binding agents, we screened a ~72,000-member library of small molecules for ability to displace ThS from tau filaments prepared from full-length human 2N4R tau protein in the presence of alkyl sulfate inducer.¹⁵ The screen identified triarylmethines and oxindoles as potent new ThS displacement agents. Along with phenothiazines, these scaffolds share a planar, fairly rigid structure that can foster highly delocalized aromatic pi-electrons when appropriately substituted with electron donating and accepting groups. As a result, certain members of these families are highly polarizable, and therefore capable of supporting strong van der Waals interactions between ligand and binding sites exposed on fibril surfaces.^{17–20} On the basis of these considerations, we proposed that compound polarizability may be an important determinant of tau fibril binding affinity.⁷ Here we test this hypothesis by investigating the structure–activity relationship of representative phenothiazine, triarylmethine, and other scaffold derivatives when interacting with both authentic and

Abbreviations: AC₅₀, half-maximal activity concentration; AD, Alzheimer's disease; ODS, octadecyl sulfate; PHF, paired helical filament; ThS, Thioflavin S; ThT, Thioflavin T.

^{*} Corresponding author. Address: OSU Center for Molecular Neurobiology, 1060 Carmack Rd., Columbus, OH 43210, USA. Tel.: +1 614 688 5899; fax: +1 614 292 5379.

E-mail address: kuret.3@osu.edu (J. Kuret).

[†] Equal contribution.

[‡] Present address: Centre for Drug Research & Development, Vancouver, Canada.

synthetic tau filaments. The results suggest that van der Waals dispersion forces contribute to tau filament binding affinity.

2. Results

2.1. Synthetic filament binding affinity correlates with binding to authentic PHF

Although synthetic tau fibrils composed of recombinant tau are useful for large-scale screening and characterization of tau-binding ligands, compounds intended for use as AD diagnostic agents must bind authentic tau lesions composed of PHF tau, which are heterogeneous structures. To test whether filament composition influenced ligand binding, **1**, **5**, **12**, **13**, and **14** (Tables 1 and 2) were assayed for their ability to displace ThS from authentic PHFs isolated from AD brain and from synthetic tau filaments prepared from a full-length four-repeat isoform of tau (2N4R). ThS was used as the probe for this experiment because it yielded higher fluorescence than ThT in the presence of PHF tau (data not shown). Recombinant 2N4R tau and octadecyl sulfate (ODS) inducer were used to prepare synthetic aggregates because full-length tau isoforms accumulate in disease,²¹ and because four repeat tau isoforms aggregate efficiently under these conditions in vitro.²² The test compounds were selected to represent four distinct scaffolds while spanning ~2 orders of magnitude in relative potency and possessing different net charges. Results showed that members of the test set displaced ThS from PHF tau with similar affinity and efficacy as from synthetic tau aggregates (shown for **12** only, Fig. 1A). When the affinity data were fit by linear regression, the correlation coefficient (R^2) was 0.92 (Fig. 1B). These data indicate that displacement screens employing synthetic ODS-induced tau aggregates are useful approximations for identifying candidate PHF-binding ligands, and that similar forces likely govern compound binding to filaments composed of either full-length recombinant or PHF tau.

2.2. Synthetic tau filament morphology weakly influences ligand affinity

Synthetic filaments can be prepared from various anionic inducers. ODS inducer generates a filament morphology similar to those induced by fatty acids⁸ but distinct from those induced by heparin.²³ To determine whether aggregation inducer influenced ligand binding affinity, the ability of **1**, **5**, **12**, **13**, and **14** were assayed in ThS displacement format using 2N4R tau aggregates prepared in the presence of either ODS, arachidonic acid, or heparin inducers. Results showed that compound potency and rank order correlated strongly between both ODS- and arachidonic acid-induced filaments, and between ODS- and heparin-induced filaments (Fig. 2). However, binding affinity for heparin-induced filaments trended toward being higher than for ODS- or arachidonic acid induced filaments (Fig. 2). These data suggest that the forces mediating binding are similar among synthetic tau aggregates, with only minor effects of aggregate morphology on the absolute quantitation of compound affinity.

2.3. Quantitation of ligand binding by thioflavin dye displacement

The forces mediating binding of compounds to synthetic tau aggregates were investigated using phenothiazine and triarylamine derivatives. These scaffolds were employed because closely related analogs were available. Both ThT and ThS were used as probes in case differences in their size and net charge^{24,25} influenced displacement assay performance. The phenothiazines shared similar molecular weights, hydrophobicity, and sterics, while varying primarily in the strength of their electron donating amine groups (compounds **1–6**; Table 1). All were found to efficiently displace ThT probe, which was used at 1 μ M final concentration, with half-maximal activity concentration (AC_{50}) values distributed over nearly two orders of magnitude (Fig. 3A). Displacement of ThS probe, which was used at 10 μ M final concentration, was less

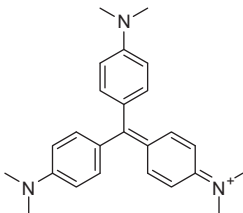
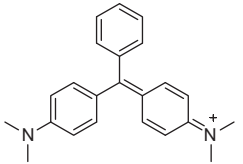
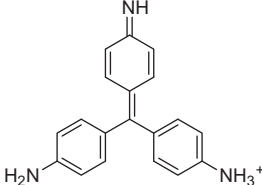
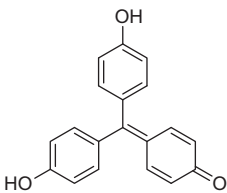
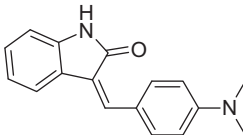
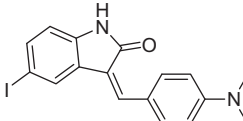
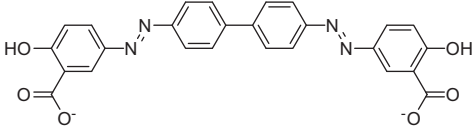
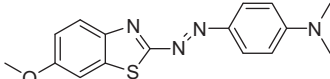
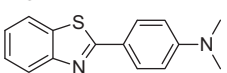
Table 1
Structure and physical properties of phenothiazine derivatives

| Compound | Structure | Salt | λ_{\max}^a (nm) | α^b (\AA^3) | $c \log P^b$ |
|-----------------------|-----------|---------------|-------------------------|-------------------------------|--------------|
| <i>Phenothiazines</i> | | | | | |
| 1 | | Cl^- | 663 | 75.5 | 0.093 |
| 2 | | Cl^- | 647 | 71.5 | -0.151 |
| 3 | | Cl^- | 632 | 69.4 | -0.149 |
| 4 | | Cl^- | 627 | 66.0 | -0.933 |
| 5 | | Cl^- | 620 | 62.0 | -0.115 |
| 6 | | Cl^- | 598 | 56.8 | -0.215 |

^a Determined by absorbance spectroscopy as described previously.⁵²

^b Calculated as described in Materials and Methods.

Table 2
Structure and physical properties of 7–15

| Compound | Structure | Salt | α (Å ³) | c log P |
|------------------------|---|------------------|----------------------------|---------|
| <i>Triarylmethines</i> | | | | |
| 7 |  | Cl [−] | 100.8 | 1.46 |
| 8 |  | Cl [−] | 86.5 | 1.36 |
| 9 |  | Cl [−] | 73.5 | −0.76 |
| 10 |  | — | 62.9 | 3.56 |
| <i>Oxindoles</i> | | | | |
| 11 |  | — | 60.1 | 3.23 |
| 12 |  | — | 67.1 | 4.30 |
| <i>Miscellaneous</i> | | | | |
| 13 |  | 2Na ⁺ | 107.4 | 3.82 |
| 14 |  | — | 79.9 | 4.82 |
| 15 |  | — | 51.9 | 4.39 |

efficient, with higher AC₅₀s reflecting the higher concentration of competing ThS probe (Fig. 3A). When the resultant AC₅₀ values were compared, the rank order of phenothiazine AC₅₀s observed with ThS correlated with those identified with ThT (Fig. 3A).

This approach was then extended to a series of four triarylmethines (compounds 7–10; Table 2), which again shared similar molecular weight and sterics, while varying only in the structure

of their ring substituents. These compounds displaced thioflavin dyes with AC₅₀ values distributed over one order of magnitude, with rank order potency correlating strongly between ThS and ThT assay formats (Fig. 3B). Together these data show that both the phenothiazine and triarylmethine series show graded potency landscapes, and that rank order of binding affinity can be detected and quantified using either ThS or ThT probes.

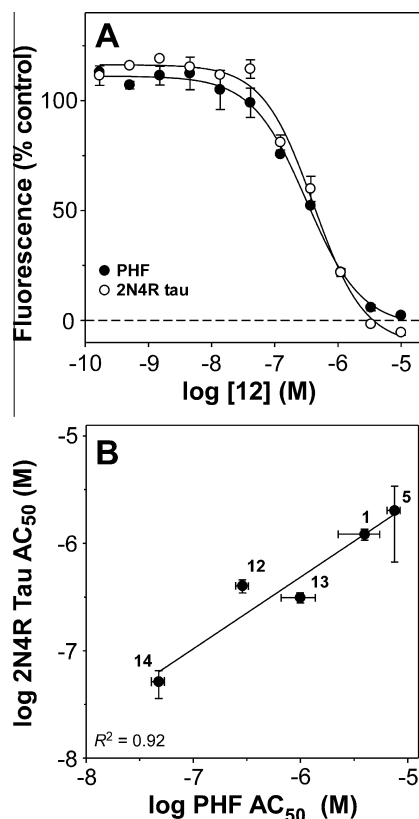


Figure 1. Synthetic tau filaments retain the ligand binding properties of authentic PHF. (A) ThS displacement assays were conducted in the presence of (●) authentic PHF and (○) synthetic tau filaments prepared in ODS inducer and varying concentrations **12**. Compound **12** displaced ThS probe completely and with submicromolar AC_{50} from both PHF and synthetic tau filaments. (B) Binding of representative ligands from different scaffold classes were tested in ThS displacement format with authentic PHFs and synthetic filaments prepared in the presence of octadecyl sulfate. Data points represent normalized AC_{50} values (\pm standard error of the estimate), with the ordinate corresponding to values determined using octadecyl sulfate-induced filaments, and the abscissa corresponding to values determined using PHFs. The solid line represents fit of data points to linear regression, with the resultant correlation coefficient reported as R^2 . Rank order of potency correlated strongly between octadecyl sulfate induced synthetic filaments and authentic PHFs.

2.4. Thioflavin dye displacement activity is mediated in part by compound polarizability

The rank order of phenothiazine potency identified above correlated directly with absorption wavelength (Table 1). This parameter reflects in part polymethine character, which fosters high compound polarizability.²⁶ To test whether polarizability was a candidate descriptor for binding affinity, the polarizability (α) of all phenothiazines and triarylmethines was directly calculated using quantum methods. For phenothiazines, the rank order of α was found to parallel the relative strengths of the electron donating groups $-N(CH_3)_2 > -NHCH_3 > -NH_2$ (attached at the 3 and 7 positions of the phenothiazine ring system) as measured by their Hammett substituent constants²⁷ (Table 1). Replots of displacement data showed a strong direct correlation between α and displacement potency in both ThS (Fig. 4A) and ThT (Fig. 4B) competition assay formats. In contrast, correlation with $c \log P$, a measure of compound hydrophobicity, was poor (Table 1). For triarylmethines, rank order of polarizability followed the substituent pattern $-N(CH_3)_2 > -NH_2 > -OH$, again consistent with Hammett substituent constants (Table 2).²⁷ Replots of these data also showed a strong direct correlation between α and displacement

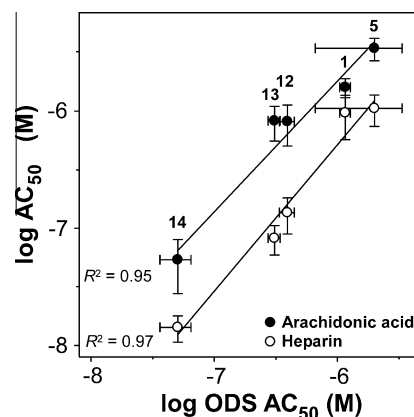


Figure 2. Synthetic tau filaments prepared in the presence of diverse inducers share ligand binding activity. Binding of representative ligands from different scaffold classes were tested in ThS displacement format with synthetic filaments prepared in the presence of octadecyl sulfate, arachidonic acid, or heparin inducers. Data points represent normalized AC_{50} values (\pm standard error of the estimate), with the abscissa corresponding to values determined using octadecyl sulfate-induced filaments, and the ordinate corresponding to values determined using arachidonic acid (●) or heparin (○) inducers. The solid line represents the fit of data points to linear regression, with the resultant correlation coefficient reported as R^2 . Rank order of potency correlated strongly among synthetic filament preparations, regardless of whether octadecyl sulfate, heparin, or arachidonic acid was used as inducer.

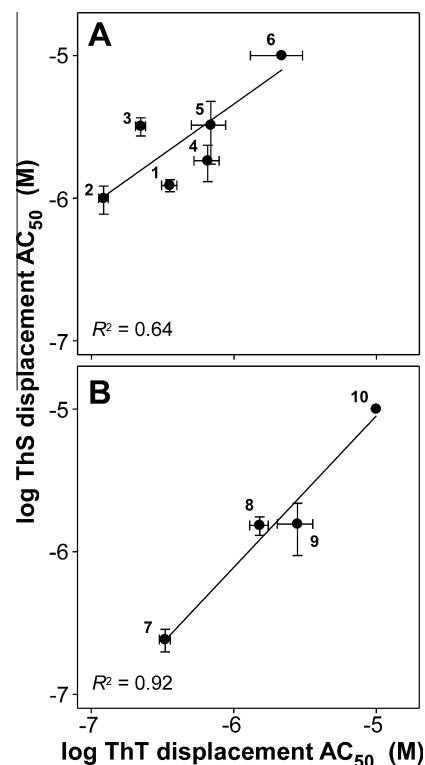


Figure 3. Displacement of thioflavin dyes from synthetic tau filaments by phenothiazine and triarylmethine derivatives. Each data point represents a normalized AC_{50} value (\pm standard error of the estimate) determined for (A) phenothiazines (1–6; Table 1) or (B) triarylmethines (7–10; Table 2) determined by displacement of ThT (abscissa) or ThS (ordinate) probes (Error bars for **10** were omitted owing to incomplete concentration effect curves). Solid lines represent best fit of the data to linear regression, with the resultant correlation coefficient reported as R^2 . Compound affinity estimated by ThS displacement assays correlated with those estimated by ThT displacement assay despite differences in the size and net charge of these probes.

potency in both ThS (Fig. 4C) and ThT (Fig. 4D) competition assay formats. Unlike phenothiazines, the triarylmethines varied greatly

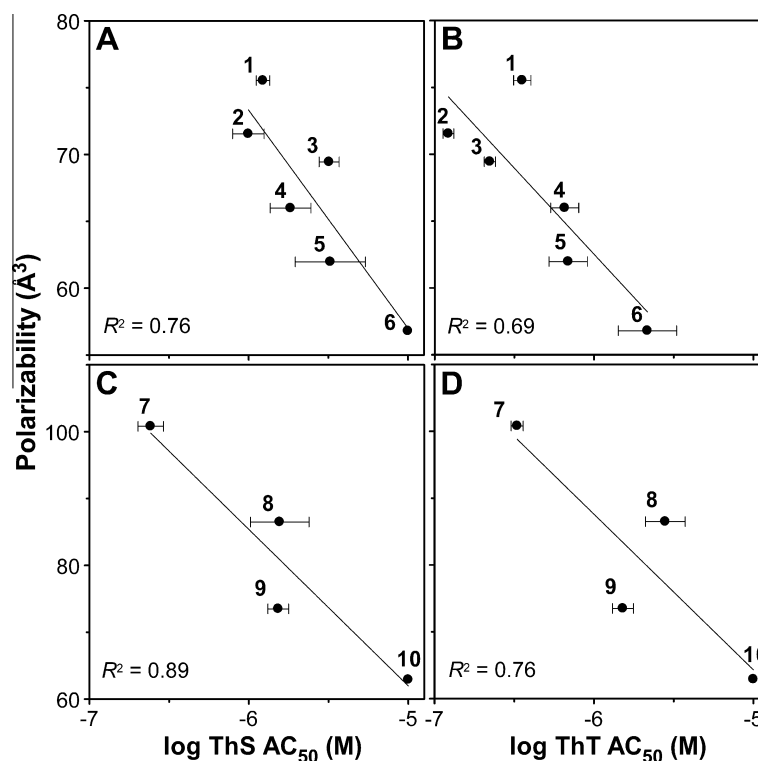


Figure 4. Binding affinity of synthetic tau filaments for phenothiazines and triarylmethines correlate with compound polarizability. Data points represent normalized AC₅₀ values (\pm standard error of the estimate) determined for (A, B) phenothiazines (1–6; Table 1) or (C, D) triarylmethines (7–10; Table 2) using ThS (A, C) or ThT (B, D) displacement assay formats (error bars for **10** were omitted owing to incomplete concentration effect curves). Solid lines represent best fit of the data to linear regression, with the resultant correlation coefficient reported as R^2 . Compound affinity correlated with polarizability calculated by ab initio methods.

in $c \log P$, yet no correlation between compound potency and hydrophobicity could be detected (Table 2). Together these data are consistent with compound polarizability being an important determinant of binding affinity in two structurally distinct tau aggregate binding scaffolds.

2.5. Tau filaments present multiple binding sites for small molecules

Computational modeling studies have predicted that ThT probe interacts with cross- β -sheet aggregates through multiple binding modes that become occupied at different probe concentrations.^{28,29} To determine whether tau aggregates also support multimodal binding, synthetic ON4R tau filaments prepared in ODS inducer were incubated with varying concentrations (17 pM–10 μ M) of either **11** (an oxindole) or **15** (a benzothiazole) in the presence of varying concentrations of ThT probe (0.1–12.8 μ M). These compounds were chosen for analysis because their neutral charge at physiological pH and small size made them the most drug like of compounds identified through screening.¹⁵ In fact, certain benzothiazole and oxindole derivatives are under investigation for imaging applications.^{5,30} In addition, we previously showed that benzothiazoles such as **15**, but not oxindole **11**, were partial antagonists of ThS binding,³¹ suggesting that these two scaffolds potentially interacted differently with tau aggregates. Results confirmed that increasing concentrations of **11** were capable of completely displacing the lowest concentration of ThT probe (Fig. 5A). As ThT concentrations were increased, **11** remained capable of complete displacement, but with steadily increasing apparent AC₅₀ (Fig. 5A). This behavior is typical of a competitive binding mechanism, and suggests that **11** displaced ThT from all binding modes associated with the fluorescence wavelengths used in this

study. When **15** was examined in the same experimental paradigm, it too completely displaced the lowest concentration of ThT probe (Fig. 5B). In this case, however, the displacement efficacy of **15** steadily decreased with increasing ThT probe concentration (Fig. 5B), suggesting it was incapable of displacing ThT from sites that became occupied at high probe concentrations. These data suggest that recombinant tau filaments present at least two distinct ThT binding sites that can be occupied at different probe concentrations, and that the ability of ligands to displace ThT depends on which probe sites are occupied. Overall, these data indicate that the binding trends identified herein apply only to a subset of tau binding sites, and that these are best investigated at low thioflavin probe concentrations.

3. Discussion

Cross- β -sheet aggregates, including tau filaments, represent non-canonical binding targets for small molecules because they lack deep pockets normally associated with high-affinity, stereospecific binding. Instead, they present narrow, solvent exposed channels that extend along their surfaces.⁷ Despite the lack of a 'lock and key' rationale for ligand binding, certain small molecules do bind tau protein aggregates with high affinity.¹⁵ These molecules are members of seemingly unrelated scaffold classes, yet share planar structure and positioning of electron donating substituents that maximize ligand polarizability. Because many aggregate binding dyes possess negative or positive net charge, it has been proposed that charge–charge interactions dominate binding.³² However, the net charge associated with the phenothiazines and triarylmethines investigated herein is highly delocalized across the entire molecule, which adopts the alternating π -electron density distribution of the polymethine state.³³ This electronic

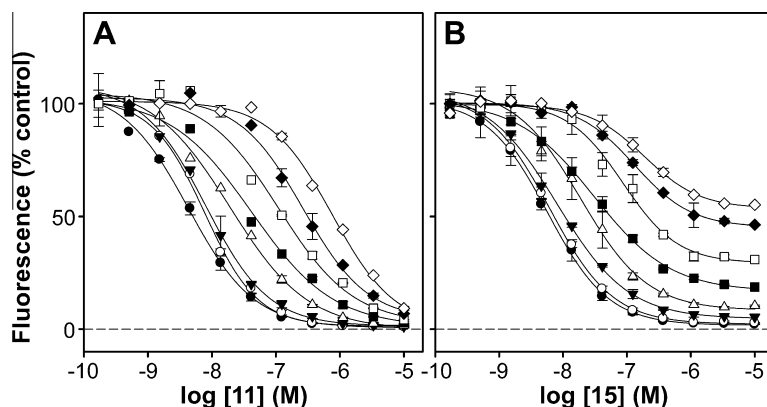


Figure 5. Synthetic tau filaments present multiple binding sites. ThT displacement assays were conducted in the presence of synthetic tau filaments and varying concentrations of ThT probe (0.1, ●; 0.2, ○; 0.4, ▼; 0.8, △; 1.6, ■; 3.2, □; 6.4, ◆; and 12.8 μ M, ◇) and compounds (A) **11**, and (B), **15** (each varied from 17 pM–10 μ M final concentration). Data points represent normalized fluorescence intensities (\pm SD of triplicate determination), whereas solid lines represent fits of data points to Eq. 1. Under these conditions, **11** displaced ThT probe completely at all ThT concentrations, whereas **15** was a partial displacer at higher ThT concentrations.

structure is associated with absorption at visible wavelengths, high extinction coefficients, and high molecular polarizability.³³ The results presented herein suggest that polarizability is an important descriptor of tau filament binding affinity for these ligands. We were able to detect its contribution by examining closely related analogs within phenothiazine and triarylmethine scaffold families, in which other potential descriptors such as net charge, surface area, sterics, charge, hydrophobicity, and number of rotatable bonds could be held constant or controlled within narrow limits. Under these conditions, positive correlations were observed between binding affinity as measured by thioflavin dye displacement assay and polarizability calculated by *ab initio* methods. A quantum approach was necessary because polarizability is not well resolved among closely related compounds in most semi-empirical scoring approaches.³⁴ Although binding affinity correlated with polarizability within scaffold families, correlation was lost when the series were merged or compounds from multiple structural classes were combined (data not shown). These data suggest that additional factors beyond polarizability also contribute to tau filament binding affinity, and that larger quantitative structure–activity relationship studies will be required to identify them. Moreover, entropic contributions to binding may be important, as shown recently for dye–textile interactions.³⁵ The results presented herein indicate that synthetic tau aggregates will be an appropriate substrate for identifying additional descriptors for binding authentic PHFs, which are not available in sufficient quantities to conduct screens or detailed characterization studies.

Compound polarizability (α) describes how easily electron density can shift about the molecule when exposed to an external electric field, such as from a nearby dipole or ion.³⁶ It is a potential mediator of small molecule binding affinity to tau fibrils because it can support strong van der Waals dispersion interactions with planar binding surfaces. Recent computational models of benzothiazole binding to cross- β -sheet aggregates identified multiple hypothetical modes of interaction that could leverage dispersion forces.³⁷ One identified high-affinity site is located in channels that expose the hydrogen-bonding network of the β -sheet mainchain amides to solvent.²⁸ The electrons in these networks are highly delocalized and generate a dipole oriented along the filament long axis. Indeed, cross- β -sheet protein aggregates are semiconductors.³⁸ Dispersion interactions between ligand and this H-bonding network would not only contribute binding energy, but would help orient ligands so that their dipoles, which are generally oriented along their long axes, align parallel to the filament dipole. This orientation has been observed experimentally when dye molecules

such as Congo red or Michler's hydrol blue bind cross- β -sheet aggregates.^{39,40} Other, potentially lower affinity binding sites have been proposed to reside along hydrophobic clefts formed by in-register aromatic side chains.²⁹ Dispersion forces between ligands and these sites may be weaker, however, owing to dynamic movement of the side chains. Although these specific modes of binding have not been reported for tau filaments, we found that synthetic tau filaments do present multiple binding sites, only a subset of which associate with Stokes shift of the ThT probe. These results rationalize our observation of partial displacement of thioflavin probe by certain ligands.¹⁵ In future characterization of ligand displacement, it will be important to keep thioflavin probe concentration as low as possible to facilitate detection of high-affinity binding.

In summary, we propose that polarizability is an important commonality among tau aggregate binding ligands, and a potentially useful consideration in the design of new tau-directed contrast agents. The small size and neutral charge of benzothiazole and oxindole scaffolds make them well suited for this purpose.

4. Experimental procedures

4.1. Materials

Recombinant human tau proteins were prepared and stored as previously described.^{41,42} ThS, ThT, N-laurylsarcosine, heparin, and compounds **1–11** were purchased from Sigma-Aldrich (St. Louis, MO). Compound **12** was obtained from Avid Pharmaceuticals (Philadelphia, PA), **13** from AnaSpec (Fremont, CA), **14** was from Chembridge (San Diego, CA), and **15** and **16** from the NIH Chemical Genomics Center (Rockville, MD). ODS was from Research Plus (Bayonne, NJ). All compounds were used as supplied.

4.2. Isolation of PHFs

Authentic PHFs were purified from an autopsy sample of temporal cortex from an AD patient's brain (Ohio State University Brain Bank, Columbus, OH) using a modification of two procedures.^{43,44} Briefly, after cutting away and discarding the white matter, the gray matter was minced and homogenized with a blender in five volumes of a buffer containing 20 mM MES/NaOH, pH 6.8, 80 mM NaCl, 1 mM $MgCl_2$, 2 mM EGTA, 0.1 mM EDTA and 1 mM PMSF. The mixture was further homogenized in a Teflon/glass homogenizer with a Fisher Scientific model LR400C stirrer and centrifuged at 27,000 $\times g$ for 20 min at 4 $^{\circ}C$. After discarding

the supernatant, the pellet was resuspended in 10 volumes of 0.8 M NaCl, 10% sucrose, 10 mM MES/NaOH, pH 7.4, 1 mM EGTA and 0.1 mM PMSF, and rehomogenized and centrifuged as above. After discarding the pellet, the supernatant was incubated with 1% N-laurylsarcosine (w/v) for 1 h at room temperature on an orbital shaker. The mixture was then centrifuged at 87,000×g for 35 min at 4 °C and the supernatant was discarded. The pellet was resuspended in 10 mM MES/NaOH, pH 7.0 (0.2 mL/g tissue) and added (9.25 mL/tube) to 40 mL, thin-walled polyallomer tubes containing a discontinuous sucrose gradient constructed from 9.25 mL layers of 1 M, 1.5 M, and 2 M sucrose in 10 mM MES/NaOH pH 7.0. The tubes were centrifuged at 112,600×g for 2 h and 25 min at 4 °C and the layers were removed from the top and examined by transmission electron microscopy by an established protocol.⁴⁵ The fraction containing the PHFs was then stored in aliquots at –80 °C until needed.

4.3. Displacement assays

ThS and ThT displacement fluorescence assays were performed as described previously.¹⁵ Controls without compound and without protein were included on each plate. Each compound was tested at least twice in duplicate. Fluorescence was measured at $\lambda_{\text{ex}} = 440$ nm; $\lambda_{\text{em}} = 490$ nm; filter = 475 nm in a FlexStation plate reader (Molecular Devices, Sunnyvale, CA) operated at 10 reads/well and PMT on the highest setting.

Thioflavin dye displacement was determined by subtracting the fluorescence of wells without protein from those containing protein and compound (net fluorescence). Percent control ThS or ThT fluorescence was then calculated by dividing net fluorescence by the values of wells containing protein but no competitive compound. The data were then fit to the function:

$$F = F_{\min} + \frac{F_{\max} - F_{\min}}{1 + 10^{(AC_{50} - x)^n}} \quad (1)$$

where F is the ThS or ThT fluorescence in the presence of compound, F_{\min} is the fluorescence at infinite compound concentration, F_{\max} is the ThS or ThT fluorescence with no competitive compound, AC_{50} is the concentration of competitive compound that reduces the ThS or ThT fluorescence by 50%, and n is the Hill coefficient.

4.4. Computational chemistry

All compounds were built using Chem3D Pro 12.0 software⁴⁶ and minimized using Allinger's molecular mechanics MM2 force field⁴⁷ (default convergence criteria minimum RMS gradient 0.1 and 10,000 iterations). Polarizability (α) for each structure was calculated at the quantum level using theoretical methods implemented in Gaussian 09 (G09)⁴⁸ software package and the calculations were performed on the Ohio Supercomputing Center clusters. Each compound structure was evaluated using the three-step approach of Perpete et al.^{49,50} consisting of: (i) a ground-state geometry optimization with 3×10^{-4} a.u. residual mean square convergence criteria (default OPT threshold); (ii) confirmation of ground-state geometry with vibrational spectrum determination (structure minima verified by real vibrational frequencies); (iii) calculation of α in a static ($\omega = 0$) external electric field (default 1 a.u. in principal axes), at the optimized ground-state geometry. All calculations were performed with the hybrid Density Functional Theory functional B3LYP with basis set 6-311++G(d,p). Bulk solvent effects were implicitly modeled with the polarizable continuum model⁵¹ (G09 keywords SCRF = (Solvent = Methanol)). Polarizabilities are reported as the mean, $\langle\alpha\rangle$, or the average of the three polarizability tensor quantities that

correspond to x , y , and z components of parallel external field principal axes:³⁶

$$\langle\alpha\rangle = \frac{1}{3}(\alpha_{xx} + \alpha_{yy} + \alpha_{zz}) \quad (2)$$

given in units of polarizability volume (\AA^3).

Clog P values for the structures shown in Tables 1 and 2 (neglecting counterions) were estimated using the highly parameterized and robustly trained fragment-based algorithm of the Molinspiration Property Calculation Service (<http://www.molinspiration.com>).

Acknowledgments

We thank Dr. Douglas W. Scharre for access to the Buckeye Brain Bank, Drs. Mike X. Zhu and Dennis B. McKay for access to FlexStation plate readers, and Avid radiopharmaceuticals for their gift of compound 16. This work was supported by a grant from the Alzheimer's Drug Discovery Foundation (281205) and an allocation of computing time from the Ohio Supercomputer Center (PAS0453).

References and notes

- Mebane-Sims, I. *Alzheimer's Dement.* **2009**, 5, 234.
- Hebert, L. E.; Scherr, P. A.; Bienias, J. L.; Bennett, D. A.; Evans, D. A. *Arch. Neurol.* **2003**, 60, 1119.
- Kuret, J. In *Protein folding diseases: enzyme inhibitors and other agents as prospective therapies*; Smith, H. J., Sewell, R. D. E., Simons, C., Eds.; CRC Press, Taylor & Francis Books: Boca Raton, FL, 2007; Vol. 5, p 287.
- Choi, S. R.; Golding, G.; Zhuang, Z.; Zhang, W.; Lim, N.; Hefti, F.; Benedum, T. E.; Kilbourn, M. R.; Skovronsky, D.; Kung, H. F. *J. Nucl. Med.* **2009**, 50, 1887.
- Nelissen, N.; Van Laere, K.; Thurfjell, L.; Owenius, R.; Vandenbulcke, M.; Koole, M.; Bormans, G.; Brooks, D. J.; Vandenberghe, R. J. *Nucl. Med.* **2009**, 50, 1251.
- Rowe, C. C.; Ackerman, U.; Browne, W.; Mulligan, R.; Pike, K. L.; O'Keefe, G.; Tochon-Danguy, H.; Chan, G.; Berlangieri, S. U.; Jones, G.; Dickinson-Rowe, K. L.; Kung, H. P.; Zhang, W.; Kung, M. P.; Skovronsky, D.; Dyrks, T.; Holl, G.; Krause, S.; Friebe, M.; Lehman, L.; Lindemann, S.; Dinkelborg, L. M.; Masters, C. L.; Villemagne, V. L. *Lancet Neurol.* **2008**, 7, 129.
- Jensen, J. R.; Cisek, K.; Funk, K. E.; Naphade, S.; Schafer, K.; Kuret, J. *J. Alzheimers Dis.* **2011**, 26.
- Chirita, C. N.; Necula, M.; Kuret, J. *J. Biol. Chem.* **2003**, 278, 25644.
- Perez, M.; Valpuesta, J. M.; Medina, M.; Montejo de Garcini, E.; Avila, J. *J. Neurochem.* **1996**, 67, 1183.
- Wilson, D. M.; Binder, L. I. *Am. J. Pathol.* **1997**, 150, 2181.
- Friedhoff, P.; Schneider, A.; Mandelkow, E. M.; Mandelkow, E. *Biochemistry* **1998**, 37, 10223.
- King, M. E.; Ahuja, V.; Binder, L. I.; Kuret, J. *Biochemistry* **1999**, 38, 14851.
- Kemp, S.; Storey, L.; Storey, J.; Rickard, J.; Harrington, C.; Wischik, C. UK Patent WO 2010/034982 A1, 2010.
- Appel, T. R.; Richter, S.; Linke, R. P.; Makovitzky, J. *Amyloid* **2005**, 12, 174.
- Honson, N. S.; Johnson, R. L.; Huang, W.; Ingles, J.; Austin, C. P.; Kuret, J. *Neurobiol. Dis.* **2007**, 28, 251.
- Sergeant, N.; Bretteville, A.; Hamdane, M.; Caillet-Boudin, M. L.; Grognet, P.; Bombois, S.; Blum, D.; Delacourte, A.; Pasquier, F.; Vanmechelen, E.; Schraen-Maschke, S.; Buee, L. *Expert Rev. Proteomics* **2008**, 5, 207.
- Eisenberg, D.; Nelson, R.; Sawaya, M. R.; Balbirnie, M.; Madsen, A.; Riek, C.; Sambashivan, S.; Liu, Y.; Gingery, M.; Grothe, R. *FEBS J.* **2005**, 272, 78.
- Nelson, R.; Eisenberg, D. *Curr. Opin. Struct. Biol.* **2006**, 16, 260.
- Nelson, R.; Sawaya, M. R.; Balbirnie, M.; Madsen, A. O.; Riek, C.; Grothe, R.; Eisenberg, D. *Nature* **2005**, 435, 773.
- Parsegian, V. A. *Van der Waals Forces: A Handbook for Biologists, Chemists, Engineers, and Physicists*; New York: Cambridge University Press, 2006.
- Goedert, M.; Spillantini, M. G.; Cairns, N. J.; Crowther, R. A. *Neuron* **1992**, 8, 159.
- King, M. E.; Gamblin, T. C.; Kuret, J.; Binder, L. I. *J. Neurochem.* **2000**, 74, 1749.
- Xu, S.; Brunden, K. R.; Trojanowski, J. Q.; Lee, V. M. *Alzheimers Dement.* **2010**, 6, 110.
- Kelenyi, G. J. *Histochem. Cytochem.* **1967**, 15, 172.
- Wei, J.; Wu, C.; Lankin, D.; Gulrati, A.; Valyi-Nagy, T.; Cochran, E.; Pike, V. W.; Kozikowski, A.; Wang, Y. *Curr. Alzheimer Res.* **2005**, 2, 109.
- Dahne, S. *Science* **1978**, 199, 1163.
- Hansch, C.; Leo, A.; Taft, R. W. *Chem. Rev.* **1991**, 91, 165.
- Rodriguez-Rodriguez, C.; Rimola, A.; Rodriguez-Santiago, L.; Ugliengo, P.; Alvarez-Larena, A.; Gutierrez-de-Teran, H.; Sodupe, M.; Gonzalez-Duarte, P. *Chem. Commun.* **2010**, 46, 1156.
- Wu, C.; Biancalana, M.; Koide, S.; Shea, J. E. *J. Mol. Biol.* **2009**, 394, 627.
- Kniess, T.; Bergmann, R.; Kuchar, M.; Steinbach, J.; Wuest, F. *Bioorg. Med. Chem.* **2009**, 17, 7732.

31. Abraha, A.; Ghoshal, N.; Gamblin, T. C.; Cryns, V.; Berry, R. W.; Kuret, J.; Binder, L. I. *J. Cell Sci.* **2000**, *113*, 3737.
32. Klunk, W. E.; Pettegrew, J. W.; Abraham, D. J. *J. Histochem. Cytochem.* **1989**, *37*, 1273.
33. Dähne, S. *Science* **1978**, *199*, 1163.
34. Bryce, R. A. *Future Med. Chem.* **2011**, *3*, 683.
35. Bird, J.; Brough, N.; Dixon, S.; Batchelor, S. N. *J. Phys. Chem. B* **2006**, *110*, 19557.
36. Marder, S. R.; Sohn, J. E.; Stucky, G. D. *Materials for Nonlinear Optics: Chemical Perspectives*; American Chemical Society: Washington, DC, 1991.
37. Wu, C.; Bowers, M. T.; Shea, J. E. *Biophys. J.* **2011**, *100*, 1316.
38. Del Mercato, L. L.; Pompa, P. P.; Maruccio, G.; Della Torre, A.; Sabella, S.; Tamburro, A. M.; Cingolani, R.; Rinaldi, R. *Proc. Natl. Acad. Sci. U.S.A.* **2007**, *104*, 18019.
39. Jin, L. W.; Claborn, K. A.; Kurimoto, M.; Geday, M. A.; Maezawa, I.; Sohraby, F.; Estrada, M.; Kaminsky, W.; Kahr, B. *Proc. Natl. Acad. Sci. U.S.A.* **2003**, *100*, 15294.
40. Kitts, C. C.; Beke-Somfai, T.; Norden, B. *Biochemistry* **2011**, *50*, 3451.
41. Carmel, G.; Mager, E. M.; Binder, L. I.; Kuret, J. *J. Biol. Chem.* **1996**, *271*, 32789.
42. Necula, M.; Chirita, C. N.; Kuret, J. *J. Biol. Chem.* **2003**, *278*, 46674.
43. Greenberg, S. G.; Davies, P. *Proc. Natl. Acad. Sci. U.S.A.* **1990**, *87*, 5827.
44. Ksiezak-Reding, H.; Wall, J. S. *Neurobiol. Aging* **1994**, *15*, 11.
45. Necula, M.; Kuret, J. *Anal. Biochem.* **2004**, *329*, 238.
46. Black, H. *Chem. World-UK* **2008**, *5*, 64.
47. Allinger, N. L. *J. Am. Chem. Soc.* **1977**, *99*, 8127.
48. Frisch, M. J.; Trucks, G. W.; Schlegel, H. B.; Scuseria, G. E.; Robb, M. A.; Cheeseman, J. R.; Scalmani, G.; Barone, V.; Mennucci, B.; Petersson, G. A.; Nakatsuji, H. *Gaussian, Inc.* 2009.
49. Jacquemin, D.; Perpète, E. A. *Chem. Phys. Lett.* **2006**, *429*, 147.
50. Perpète, E. A.; Jacquemin, D. *J. Mol. Struct. Theochem.* **2009**, *914*, 100.
51. Tomasi, J.; Mennucci, B.; Cammi, R. *Chem. Rev.* **2005**, *105*, 2999.
52. Chang, E.; Congdon, E. E.; Honson, N. S.; Duff, K. E.; Kuret, J. *J. Med. Chem.* **2009**, *52*, 3539.